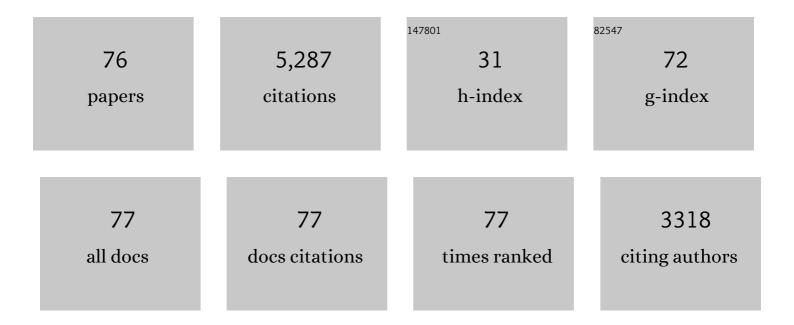
List of Publications by Year in descending order

Source: https://exaly.com/author-pdf/5959330/publications.pdf Version: 2024-02-01



AIREDT D CHEN

#	Article	IF	CITATIONS
1	Clinical translation of hyperpolarized <sup>13</sup> C pyruvate and urea MRI for simultaneous metabolic and perfusion imaging. Magnetic Resonance in Medicine, 2022, 87, 138-149.	3.0	23
2	<sup>15</sup> Nâ€carnitine, a novel endogenous hyperpolarized MRI probe with long signal lifetime. Magnetic Resonance in Medicine, 2021, 85, 1814-1820.	3.0	11
3	Characterization and compensation of inhomogeneity artifact in spiral hyperpolarized <sup>13</sup> C imaging of the human heart. Magnetic Resonance in Medicine, 2021, 86, 157-166.	3.0	8
4	Predicting response to radiotherapy of intracranial metastases with hyperpolarized \$\$^{13}\$\$C MRI. Journal of Neuro-Oncology, 2021, 152, 551-557.	2.9	15
5	Cardiac metabolic imaging using hyperpolarized [1â€< sup>13C]lactate as a substrate. NMR in Biomedicine, 2021, 34, e4532.	2.8	3
6	Monitoring Early Glycolytic Flux Alterations Following Radiotherapy in Cancer and Immune Cells: Hyperpolarized Carbon-13 Magnetic Resonance Imaging Study. Metabolites, 2021, 11, 518.	2.9	4
7	Sampling Strategies in Dynamic Hyperpolarized NMR. , 2021, , 77-102.		0
8	Lactate topography of the human brain using hyperpolarized 13C-MRI. NeuroImage, 2020, 204, 116202.	4.2	65
9	Partial Fourier reconstruction for improved resolution in 3D hyperpolarized 13 C EPI. Magnetic Resonance in Medicine, 2020, 83, 2150-2159.	3.0	2
10	Tensor image enhancement and optimal multichannel receiver combination analyses for human hyperpolarized <sup>13</sup> C MRSI. Magnetic Resonance in Medicine, 2020, 84, 3351-3365.	3.0	27
11	Correlation of hyperpolarized 13 Câ€MRI data with tissue extract measurements. NMR in Biomedicine, 2020, 33, e4269.	2.8	3
12	A multisample 7 T dynamic nuclear polarization polarizer for preclinical hyperpolarized MR. NMR in Biomedicine, 2020, 33, e4264.	2.8	24
13	Monitoring Early Changes in Tumor Metabolism in Response to Therapy Using Hyperpolarized 13C MRSI in a Preclinical Model of Glioma. Tomography, 2020, 6, 290-300.	1.8	5
14	In vivo hyperpolarization transfer in a clinical MRI scanner. Magnetic Resonance in Medicine, 2018, 80, 480-487.	3.0	7
15	Simultaneous multislice acquisition without trajectory modification for hyperpolarized <sup>13</sup> C experiments. Magnetic Resonance in Medicine, 2018, 80, 1588-1594.	3.0	11
16	Dualâ€Echo EPI sequence for integrated distortion correction in 3D timeâ€resolved hyperpolarized <sup>13</sup> C MRI. Magnetic Resonance in Medicine, 2018, 79, 643-653.	3.0	31
17	Sensitivity enhancement for detection of hyperpolarized <sup>13</sup> C MRI probes with <sup>1</sup> H spin coupling introduced by enzymatic transformation in vivo. Magnetic Resonance in Medicine, 2018, 80, 36-41.	3.0	9
18	Probing the cardiac malate–aspartate shuttle nonâ€invasively using hyperpolarized [1,2â€ <sup>13</sup> C <sub>2</sub> ]pyruvate. NMR in Biomedicine, 2018, 31, e3845.	2.8	6

#	Article	IF	CITATIONS
19	Metabolic Imaging of the Human Brain with Hyperpolarized 13C Pyruvate Demonstrates 13C Lactate Production in Brain Tumor Patients. Cancer Research, 2018, 78, 3755-3760.	0.9	179
20	Improved tolerance to offâ€resonance in spectralâ€spatial EPI of hyperpolarized [1â€ <sup>13</sup> C]pyruvate and metabolites. Magnetic Resonance in Medicine, 2018, 80, 925-934.	3.0	10
21	Exposure to a PBDE/OHâ€BDE mixture alters juvenile zebrafish ( <i>Danio rerio</i> ) development. Environmental Toxicology and Chemistry, 2017, 36, 36-48.	4.3	20
22	Accelerated 3D echoâ€planar imaging with compressed sensing for timeâ€resolved hyperpolarized <sup>13</sup> C studies. Magnetic Resonance in Medicine, 2017, 77, 538-546.	3.0	22
23	Diffusionâ€weighted Jâ€resolved spectroscopy. Magnetic Resonance in Medicine, 2017, 78, 1235-1245.	3.0	9
24	<i>T</i> <sub>1</sub> nuclear magnetic relaxation dispersion of hyperpolarized sodium and cesium hydrogencarbonateâ€ <sup>13</sup> C. NMR in Biomedicine, 2017, 30, e3749.	2.8	4
25	Voxel-by-voxel correlations of perfusion, substrate, and metabolite signals in dynamic hyperpolarized <sup>13</sup> C imaging. NMR in Biomedicine, 2016, 29, 1038-1047.	2.8	14
26	Hyperpolarized [1â€ <sup>13</sup> C]pyruvate MRI for noninvasive examination of placental metabolism and nutrient transport: A feasibility study in pregnant guinea pigs. Journal of Magnetic Resonance Imaging, 2016, 43, 750-755.	3.4	15
27	A rapid inversion technique for the measurement of longitudinal relaxation times of brain metabolites: application to lactate in highâ€grade gliomas at 3 T. NMR in Biomedicine, 2016, 29, 1381-1390.	2.8	10
28	Hyperpolarized <sup>13</sup> C Metabolic MRI of the Human Heart. Circulation Research, 2016, 119, 1177-1182.	4.5	296
29	Intensity correction for multichannel hyperpolarized <sup>13</sup> C imaging of the heart. Magnetic Resonance in Medicine, 2016, 75, 859-865.	3.0	22
30	Using [1â€ <sup>13</sup> C]lactic acid for hyperpolarized <sup>13</sup> C MR cardiac studies. Magnetic Resonance in Medicine, 2015, 73, 2087-2093.	3.0	22
31	Short-echo three-dimensional H-1 MR spectroscopic imaging of patients with glioma at 7 tesla for characterization of differences in metabolite levels. Journal of Magnetic Resonance Imaging, 2015, 41, 1332-1341.	3.4	44
32	Hyperpolarized choline as an MR imaging molecular probe: Feasibility of in vivo imaging in a rat model. Journal of Magnetic Resonance Imaging, 2015, 41, 917-923.	3.4	13
33	Single voxel localization for dynamic hyperpolarized 13C MR spectroscopy. Journal of Magnetic Resonance, 2015, 258, 81-85.	2.1	10
34	Frequency correction method for improved spatial correlation of hyperpolarized <sup>13</sup> C metabolites and anatomy. NMR in Biomedicine, 2014, 27, 212-218.	2.8	17
35	Mapping metabolic changes associated with early Radiation Induced Lung Injury post conformal radiotherapy using hyperpolarized 13C-pyruvate Magnetic Resonance Spectroscopic Imaging. Radiotherapy and Oncology, 2014, 110, 317-322.	0.6	31
36	Reproducibility study for freeâ€breathing measurements of pyruvate metabolism using hyperpolarized <sup>13</sup> C in the heart. Magnetic Resonance in Medicine, 2013, 69, 1063-1071.	3.0	24

#	Article	IF	CITATIONS
37	Multichannel receiver coils for improved coverage in cardiac metabolic imaging using prepolarized <sup>13</sup> C substrates. Magnetic Resonance in Medicine, 2013, 70, 295-300.	3.0	12
38	Metabolic Imaging of Patients with Prostate Cancer Using Hyperpolarized [1- <sup>13</sup> C]Pyruvate. Science Translational Medicine, 2013, 5, 198ra108.	12.4	1,061
39	Hyperpolarized <sup>13</sup> C magnetic resonance reveals early―and lateâ€onset changes to <i>in vivo</i> pyruvate metabolism in the failing heart. European Journal of Heart Failure, 2013, 15, 130-140.	7.1	133
40	A calibrationâ€based approach to realâ€ŧime <i>in vivo</i> monitoring of pyruvate C <sub>1</sub> and C <sub>2</sub> polarization using the <i>J</i> <sub>CC</sub> spectral asymmetry. NMR in Biomedicine, 2013, 26, 1233-1241.	2.8	11
41	Probing Early Tumor Response to Radiation Therapy Using Hyperpolarized [1-13C]pyruvate in MDA-MB-231 Xenografts. PLoS ONE, 2013, 8, e56551.	2.5	32
42	Hyperpolarized <sup>13</sup> C metabolic imaging using dissolution dynamic nuclear polarization. Journal of Magnetic Resonance Imaging, 2012, 36, 1314-1328.	3.4	98
43	Optimisation of dynamic nuclear polarisation of [1-13C] pyruvate by addition of gadolinium-based contrast agents. Journal of Magnetic Resonance, 2012, 223, 85-89.	2.1	26
44	Spin tagging for hyperpolarized 13C metabolic studies. Journal of Magnetic Resonance, 2012, 214, 319-323.	2.1	11
45	Simultaneous investigation of cardiac pyruvate dehydrogenase flux, Krebs cycle metabolism and pH, using hyperpolarized [1,2â€ <sup>13</sup> C <sub>2</sub> ]pyruvate <i>in vivo</i> . NMR in Biomedicine, 2012, 25, 305-311.	2.8	65
46	Integrated Blochâ€ <b>s</b> iegert <i>B</i> <sub>1</sub> mapping and multislice imaging of hyperpolarized <sup>13</sup> C pyruvate and bicarbonate in the heart. Magnetic Resonance in Medicine, 2012, 67, 62-71.	3.0	28
47	Implementation of 3ÂT Lactate-Edited 3D 1H MR Spectroscopic Imaging with Flyback Echo-Planar Readout for Gliomas Patients. Annals of Biomedical Engineering, 2011, 39, 193-204.	2.5	35
48	<sup>13</sup> C MR reporter probe system using dynamic nuclear polarization. NMR in Biomedicine, 2011, 24, 514-520.	2.8	32
49	Spectral–spatial excitation for rapid imaging of DNP compounds. NMR in Biomedicine, 2011, 24, 988-996.	2.8	70
50	Investigation of tumor hyperpolarized [1- <sup> <b>13</b> </sup> C]-pyruvate dynamics using time-resolved multiband RF excitation echo-planar MRSI. Magnetic Resonance in Medicine, 2010, 63, 582-591.	3.0	85
51	Metabolic imaging in the anesthetized rat brain using hyperpolarized [1â€ <sup>13</sup> C] pyruvate and [1â€ <sup>13</sup> C] ethyl pyruvate. Magnetic Resonance in Medicine, 2010, 63, 1137-1143.	3.0	117
52	Rapid multislice imaging of hyperpolarized <sup>13</sup> C pyruvate and bicarbonate in the heart. Magnetic Resonance in Medicine, 2010, 64, 1323-1331.	3.0	144
53	Analysis of hyperpolarized dynamic 13C lactate imaging in a transgenic mouse model of prostate cancer. Magnetic Resonance Imaging, 2010, 28, 153-162.	1.8	48
54	Kinetic modeling of hyperpolarized 13C1-pyruvate metabolism in normal rats and TRAMP mice. Journal of Magnetic Resonance, 2010, 202, 85-92.	2.1	160

#	Article	IF	CITATIONS
55	Multi-compound polarization by DNP allows simultaneous assessment of multiple enzymatic activities in vivo. Journal of Magnetic Resonance, 2010, 205, 141-147.	2.1	154
56	Generation of hyperpolarized substrates by secondary labeling with [1,1-13C] acetic anhydride. Proceedings of the National Academy of Sciences of the United States of America, 2009, 106, 5503-5507.	7.1	46
57	In vivo hyperpolarized 13C MR spectroscopic imaging with 1H decoupling. Journal of Magnetic Resonance, 2009, 197, 100-106.	2.1	32
58	In Vivo Carbon-13 Dynamic MRS and MRSI of Normal and Fasted Rat Liver with Hyperpolarized 13C-Pyruvate. Molecular Imaging and Biology, 2009, 11, 399-407.	2.6	64
59	3D sensitivity encoded ellipsoidal MR spectroscopic imaging of gliomas at 3T. Magnetic Resonance Imaging, 2009, 27, 1249-1257.	1.8	21
60	Design of spectral-spatial outer volume suppression RF pulses for tissue specific metabolic characterization with hyperpolarized 13C pyruvate. Journal of Magnetic Resonance, 2009, 200, 344-348.	2.1	27
61	Hyperpolarized [2- <sup>13</sup> C]-Fructose: A Hemiketal DNP Substrate for In Vivo Metabolic Imaging. Journal of the American Chemical Society, 2009, 131, 17591-17596.	13.7	106
62	Feasibility of using hyperpolarized [1-13C]lactate as a substrate for in vivo metabolic 13C MRSI studies. Magnetic Resonance Imaging, 2008, 26, 721-726.	1.8	104
63	Dynamic contrast-enhanced MRI and MR diffusion imaging to distinguish between glandular and stromal prostatic tissues. Magnetic Resonance Imaging, 2008, 26, 1071-1080.	1.8	100
64	Pulse sequence for dynamic volumetric imaging of hyperpolarized metabolic products. Journal of Magnetic Resonance, 2008, 193, 139-146.	2.1	116
65	Multiband excitation pulses for hyperpolarized 13C dynamic chemical-shift imaging. Journal of Magnetic Resonance, 2008, 194, 121-127.	2.1	141
66	Phased array 3D MR spectroscopic imaging of the brain at 7 T. Magnetic Resonance Imaging, 2008, 26, 1201-1206.	1.8	20
67	Hyperpolarized 13C Lactate, Pyruvate, and Alanine: Noninvasive Biomarkers for Prostate Cancer Detection and Grading. Cancer Research, 2008, 68, 8607-8615.	0.9	527
68	Hyperpolarized Câ€13 spectroscopic imaging of the TRAMP mouse at 3T—Initial experience. Magnetic Resonance in Medicine, 2007, 58, 1099-1106.	3.0	190
69	High-speed 3T MR spectroscopic imaging of prostate with flyback echo-planar encoding. Journal of Magnetic Resonance Imaging, 2007, 25, 1288-1292.	3.4	50
70	Double spin-echo sequence for rapid spectroscopic imaging of hyperpolarized 13C. Journal of Magnetic Resonance, 2007, 187, 357-362.	2.1	143
71	TE-Averaged two-dimensional proton spectroscopic imaging of glutamate at 3 T. NeuroImage, 2006, 30, 1171-1178.	4.2	67
72	Spectroscopic imaging of the brain with phased-array coils at 3.0 T. Magnetic Resonance Imaging, 2006, 24, 69-74.	1.8	17

#	Article	IF	CITATIONS
73	Considerations in applying 3D PRESS H-1 brain MRSI with an eight-channel phased-array coil at 3 T. Magnetic Resonance Imaging, 2006, 24, 1295-1302.	1.8	33
74	High-resolution 3D MR spectroscopic imaging of the prostate at 3 T with the MLEV-PRESS sequence. Magnetic Resonance Imaging, 2006, 24, 825-832.	1.8	52
75	Design of flyback echo-planar readout gradients for magnetic resonance spectroscopic imaging. Magnetic Resonance in Medicine, 2005, 54, 1286-1289.	3.0	91
76	Hyperpolarized Nuclear Magnetic Resonance Spectroscopy: A New Method for Metabolomic Research. , 0, , 446-471.		0